



HAL
open science

VIBRATIONAL ENERGY SCAVENGING WITH SI TECHNOLOGY ELECTROMAGNETIC INERTIAL MICROGENERATORS

C. Serre, A. Pérez-Rodriguez, N. Fondevilla, J.-R. Morante, J. Montserrat, J.
Esteve

► **To cite this version:**

C. Serre, A. Pérez-Rodriguez, N. Fondevilla, J.-R. Morante, J. Montserrat, et al.. VIBRATIONAL ENERGY SCAVENGING WITH SI TECHNOLOGY ELECTROMAGNETIC INERTIAL MICROGENERATORS. DTIP 2006, Apr 2006, Stresa, Lago Maggiore, Italy. 6 p. hal-00189301

HAL Id: hal-00189301

<https://hal.science/hal-00189301>

Submitted on 20 Nov 2007

HAL is a multi-disciplinary open access archive for the deposit and dissemination of scientific research documents, whether they are published or not. The documents may come from teaching and research institutions in France or abroad, or from public or private research centers.

L'archive ouverte pluridisciplinaire **HAL**, est destinée au dépôt et à la diffusion de documents scientifiques de niveau recherche, publiés ou non, émanant des établissements d'enseignement et de recherche français ou étrangers, des laboratoires publics ou privés.

VIBRATIONAL ENERGY SCAVENGING WITH SI TECHNOLOGY ELECTROMAGNETIC INERTIAL MICROGENERATORS

C. Serre¹, A. Pérez-Rodríguez¹, N. Fondevilla¹, J.R. Morante¹, J. Montserrat², and J. Esteve².

¹EME/CEMIC/CERMAE—Dept. Electrònica, Univ. Barcelona, Martí Franquès 1, 08028 Barcelona, Spain.

²Centre Nacional de Microelectrònica CNM-CSIC, Campus UAB, 08193 Bellaterra, Spain

ABSTRACT

In this work, we present the design and optimization of an electromagnetic inertial microgenerator for energy scavenging applications, compatible with Si technology. It consists of a fixed micromachined coil and a movable magnet (inertial mass) mounted on a resonant structure (Kapton® membrane). The modeling of the device, based on a velocity damped resonator, includes the losses related to the coil series resistance and has allowed the analysis of the design and loading conditions required to optimize both the generated power and output voltage. The characterization of a first (not optimized) prototype has allowed the validation of the model, which is then used as a roadmap for a number of optimizations for the final device design. For this design, the model developed shows the possibility to achieve power levels up to hundreds of μW 's, with voltage levels compatible with the requirements of standard rectifying circuits.

1. INTRODUCTION

The autonomy requirements of modern microsystems for wearable, ubiquitous and self-powered applications have raised an increasing demand for the development of power supplies suitable for their integration with next generation of micro and nanosensors. On the other hand, owing to the miniaturization of the devices, the power consumption have considerably decreased, allowing to consider powering alternatives based on harvesting "residual" ambient energy. Among other sources, mechanical vibrations inherent in our environment -- from the movement of our bodies to the hum of a computer -- can account for a permanent power density. This residual ambient energy can be harnessed to generate electrical power. For such applications, an interesting option is the use of inertial microgenerators for energy scavenging from the vibrations in the environment [1, 2]. These devices constitute perpetual energy sources without the need for refilling, thus being well suited for abandoned sensors, wireless systems or microsystems which must be

completely embedded within the structure, with no outside physical connections.

This work describes the design and optimization of an electromagnetic inertial microgenerator for energy scavenging applications, compatible with Si technology. The design is based on a velocity damped resonator, which is suitable for harvesting of mechanical energy from vibrations induced by operating machines and engines. These vibrations are characterized by a well defined frequency and low displacement amplitudes [3]. Adjusting the resonant frequency of the system to that of the vibrations allows to amplify these low amplitude displacements. Moreover, for these applications, the use of an electromagnetic device has the potential advantages of a high level of compatibility with Si Microsystem technology, as well as the possibility of relatively high electromechanical coupling with simple designs. The device proposed in this work has a simplified structure formed by a fixed coil and a movable magnet (inertial mass) mounted on a resonant structure (Kapton® membrane). The modeling and optimization, based on the calculation of the em damping coefficient [1], and performed by Finite elements analysis (ANSYS) are presented. The mechanical and electrical characterization of a preliminary prototype is compared to those expected with a next prototype including some of the proposed optimizations. The results obtained point out the compatibility of this simple device structure with the generation of power values up to hundreds of μW 's, with voltage levels compatible with the requirements of standard rectifying circuits.

2. DEVICE MODELLING

The modeling of the device is based on a velocity damped resonator, as represented in figure 1. This system is formed by an inertial mass m linked to the frame with an elastic constant k . The movement is damped by two forces related to the electromechanical transductor ($F_g = D_g \dot{z}$) and to a parasitic damping ($F_p = D_p \dot{z}$) due to air resistance and hysteresis loss effects in the mechanical resonator.

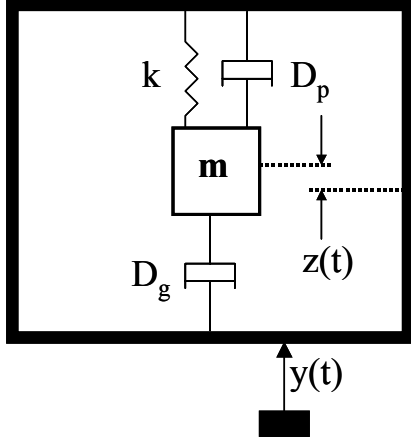


Figure 1. Schematic representation of a velocity damped resonator.

Under an harmonic excitation $y(t) = Y_o \cos(\omega t)$, the amplitude Z_o of the response is given by the module of the transfer function as follows:

$$\frac{Z_o}{Y_o} = \frac{\omega_c^2}{\sqrt{(1 - \omega_c^2)^2 + (2\zeta\omega_c)^2}} \quad (1)$$

where ζ represents the total damping coefficient $\zeta = \zeta_p + \zeta_g$, $\zeta_g = D_g/(2m\omega_n)$ and $\zeta_p = D_p/(2m\omega_n)$ are the normalized electromagnetic and parasitic damping factors, respectively, and ω_c is the angular frequency normalized to the system natural frequency ω_n .

A schematic representation of the proposed design is shown in figure 2. Assuming a resistive load, the device behaves as an inertial resonator if the inductive component of the coil impedance is much lower than the resistance in the circuit. In this case, the power generated at resonant conditions is given by:

$$P_{res} = \frac{\zeta_g Y_o^2 \omega_n^3 m}{4(\zeta_g + \zeta_p)^2} \quad (2)$$

In this design, the normalized electromagnetic damping factor ζ_g can be expressed as follows:

$$\zeta_g = \frac{1}{2m(R_C + R_L)\omega_n} \left(\frac{d\phi}{dz} \right)^2 \quad (3)$$

where R_C and R_L are the coil series and load resistances, respectively. $(d\phi/dz)$ is the magnetic flux rate through the coil due to the magnet displacement. This model also takes into account the existence of a parasitic damping ζ_p , related to air resistance and hysteresis loss effects in the mechanical resonator.

From (2), it can be derived that one condition leading to a maximum value of P_{res} is $\zeta_g = \zeta_p$. However, this doesn't

takes into account the power dissipated in the coil series resistance, which determines that only a fraction P_L of the power given by (2) is available at the load resistance. By deriving this power in relation to R_L , it is possible to determine the optimum value of R_L which maximizes P_L :

$$R_{Lopt} = \frac{1}{2m\omega_n\zeta_p} \left(\frac{d\phi}{dz} \right)^2 + R_C \quad (4)$$

which gives the following expression for the maximum power dissipated at the resistive load:

$$P_{Lopt} = \frac{Y_o^2 \omega_n^3 m}{16\zeta_p} \frac{\zeta_c}{\zeta_c + \zeta_p} \quad (5)$$

where ζ_c corresponds to the electromagnetic damping obtained with $R_L=0$. This function increases monotonously with ζ_c which, in turn, is inversely proportional to R_C . According to this, the maximum power, obtained when $R_C \rightarrow 0$, is $P_{Lmax} = [(Y_o^2 \omega_n^3 m)/(16\zeta_p)]$. Then, the optimum design in terms of the generated power corresponds to a minimum value of both R_C and ζ_p . On the other hand, the generated voltage is given by the time derivative of the magnetic flux. At resonant conditions, the voltage amplitude at the load is given by:

$$V_o = \frac{R_L}{(R_C + R_L)} \frac{Y_o \omega_n}{2(\zeta_g + \zeta_p)} \left(\frac{d\phi}{dz} \right) \quad (6)$$

In this case, the voltage increases with the value of R_L , and tends asymptotically to V_{omax} :

$$V_{omax} = \frac{Y_o \omega_n}{2\zeta_p} \left(\frac{d\phi}{dz} \right) \quad (7)$$

This implies that, in relation to R_L , the conditions leading to a maximum voltage ($R_L \rightarrow \infty$) are different from those corresponding to the maximum output power ($R_L = R_{Lopt}$).

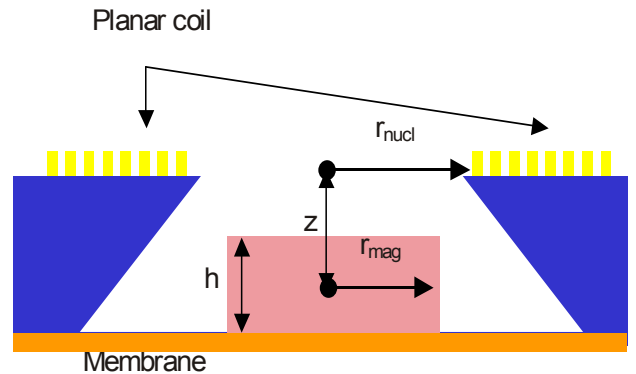


Figure 2. Schematics cross section of the device

3. FIRST PROTOTYPE FABRICATION AND CHARACTERIZATION

A first prototype has been designed and fabricated, using a coil with an area of about 1 cm^2 . The design of the device has been based on the FE analysis (ANSYS) of the flux rate $(d\phi/dz)_{\max}$ as a function of the different device parameters. This has been performed assuming coils formed by $30 \text{ }\mu\text{m}$ wide, $1.5 \text{ }\mu\text{m}$ thick Al metal tracks, with a separation between tracks of $20 \text{ }\mu\text{m}$, and for both circular and square shaped configurations. The results indicate that i) $(d\phi/dz)$ increases with the magnet size, and the optimum case is obtained when the magnet fills the whole nucleus area and ii) that there is a maximum value of the flux rate when the upper surface of the magnet is located in the plane of the coil. This analysis also shows that the optimum flux rate value for this first prototype was obtained with square shaped coils, made of 29 turns. This determines an $8 \times 8 \text{ mm}^2$ coil nucleus. A structure formed by a square shaped membrane with an inertial mass corresponding to the magnet has been implemented, using Kapton® membrane with a thickness of $127 \text{ }\mu\text{m}$. This polymer has a Young modulus significantly lower than that of Si related materials ($E = 2.5 \text{ GPa}$), which is better suited for the design of structures with resonant frequencies in the range from few Hz's to few kHz's. This has been fixed on a PCB square frame and the NdFeB permanent magnet has been glued on the centre of the membrane. To avoid potential collisions of the magnet with the edges of the coil nucleus, a magnet with a size a bit smaller than that of the nucleus has been used ($7 \times 7 \text{ mm}^2$). The characterization has been performed with the following experimental setup: excitation is provided by a piezoelectric actuator ($15 \text{ }\mu\text{m}$ displacement at 100 V), with a resonant frequency at 69 kHz (i.e. far from our

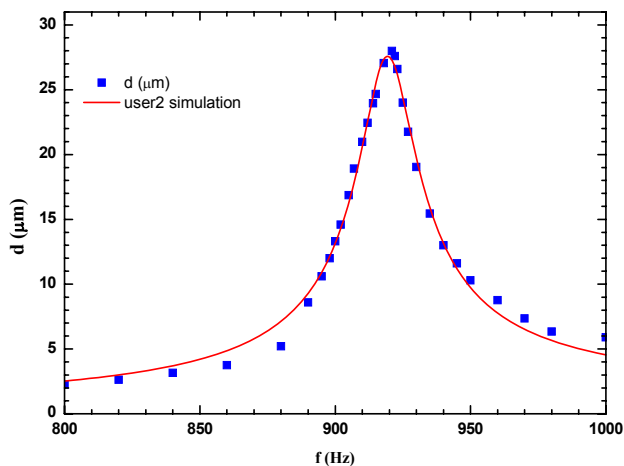


Figure 3. Mechanical characterization of the structure formed by a $7 \times 7 \times 2 \text{ mm}^3$ magnet fixed onto an $11 \times 11 \text{ mm}^2$ Kapton membrane (thickness $127 \text{ }\mu\text{m}$).

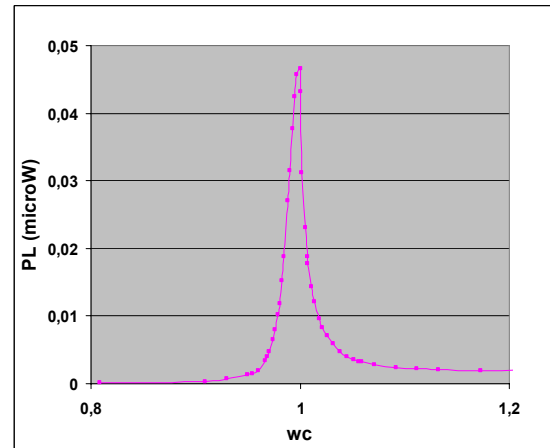


Figure 4. Output power P_L vs normalized angular frequency ω_c , measured with a load resistance $R_L = 1300 \text{ }\Omega$ and an excitation amplitude $Y_0 = 3.4 \text{ }\mu\text{m}$.

range of interest). The mechanical response of the structure is measured with a Microtak 7000 displacement sensor system coupled to a MT-250-200 laser head (MTI Instruments Inc.), allowing a vertical resolution of $0.127 \text{ }\mu\text{m}$ with a 20 kHz bandwidth. The laser head is mounted on a XYZ translation stage, and clamped to a damped mounting post to avoid noise from interaction with the excitation. The excitation signal, the analogue output of the Microtak 7000, and the electrical response of the device are monitored by an oscilloscope for easier analysis.

The mechanical characterization of this structure with an $11 \times 11 \text{ mm}^2$ membrane shows a resonant frequency (figure 3) in agreement with that simulated by ANSYS (about 920 Hz). The fitting of the experimentally measured resonant peak according to (1) has allowed to estimate the parasitic damping coefficient in this resonator to a value of $\zeta_p = 0,011$.

The electrical characterization of the microgenerator with a $7 \times 7 \times 4 \text{ mm}^3$ magnet and a $13 \times 13 \text{ mm}^2$ membrane (resonant frequency of 360 Hz , $Y_0 = 3.4 \text{ }\mu\text{m}$) is shown in figure 4. A peak power of about 45 nW was obtained. By increasing the excitation conditions up to $Y_0 = 6.8 \text{ }\mu\text{m}$, an experimental increase in the generated power up to $0.2 \text{ }\mu\text{W}$ has been obtained (higher excitation amplitudes led to non linear resonant behavior). One reason of such low power values is that in this first prototype, the $1.5 \text{ }\mu\text{m}$ thick Al metal tracks determine a high value of the coil series resistance, $R_C \approx 910 \text{ }\Omega$, which drastically limits the performance of the device.

In figure 5 and 6, the obtained data are plotted as a function of the load resistance. These data correspond to the output power and voltage amplitude measured at resonant conditions using the same excitation amplitude as in the previous figure. The figures also show the fitting of the experimental data using the theoretical equations

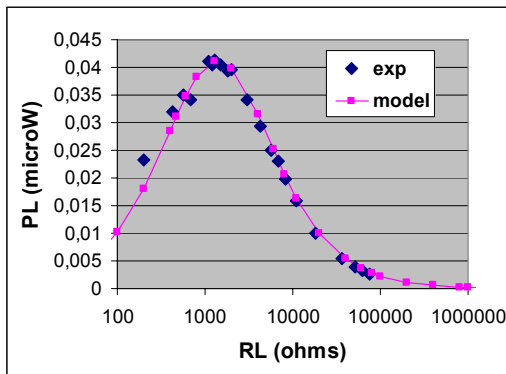


Figure 5. Output power P_L vs load resistance R_L , measured at resonant conditions.

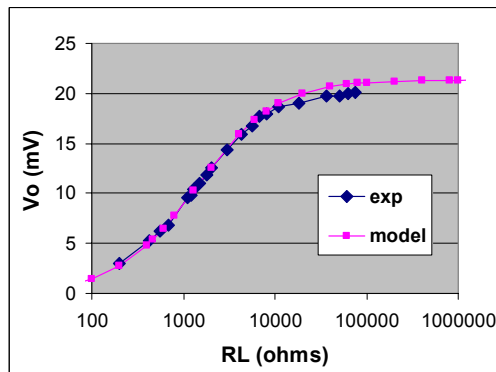


Figure 6. Output voltage V_o vs load resistance R_L , measured at resonant conditions.

described in Section 2. As shown in these figures, there is a good agreement between the experimental data and the theoretical model developed for these devices. The fitting of these data gives in this case a value of the parasitic damping $\zeta_p = 0.03$, taking into account the magnetic flux rate value of $(d\phi/dz) = 0.124$ Wb/m calculated by ANSYS for this structure. This parasitic damping is higher than that obtained from the measurements shown in figure 3, where a magnet significantly smaller was used.

These results corroborate the validity of the model developed for the electromagnetic generator. The data also show the ability of this first (not optimized) prototype to generate powers in the range between nW's and μ W's.

4. OPTIMIZATIONS

Optimizations to this design can be made in three main ways: decrease of the parasitic damping, geometric optimizations in order to maximize the magnetic flux rate $d\phi/dz$, and electric optimizations aiming at maximizing the electromagnetic coupling represented by the electromagnetic damping ζ_g .

According to equation (5) and (7), decreasing the parasitic damping in the structure allows to improve both the generated power and the output voltage. In this sense, our estimated values of ζ_p for the Kapton membranes are significantly higher than that previously reported in the literature for devices with a similar design structure ($\zeta_p = 0.0037$, [1, 4]). To minimize the parasitic damping effects, several options are being implemented, which include the fabrication of the membrane by deposition of a polymeric film (such as SU-8 or PMMA) onto a micromachined structure, and the replacement of the polyimide films by Si based membranes (which have very low mechanical hysteresis losses). A further reduction of the parasitic damping could be achieved by performing the encapsulation of the devices under vacuum conditions. However, the optimization of the device in terms of parasitic damping has also to take into account that decreasing the total damping in the system also leads to a decrease in the range of Y_o values compatible with the device design. This is determined by the existence of a higher limit Z_L for the displacement of the inertial mass in the device, imposed by the potential collision of the mass with fixed parts in the system. For a given value of Y_o , this imposes the need to have a value of total damping ($\zeta_g + \zeta_p$) $\geq [Y_o/(2Z_L)]$. To quote this value, we have made a conservative estimation of Z_L by limiting the highest vertical position of the magnet base to the position of the plane of the coil. This gives $Z_L = z + h/2$ (see figure 1), which leads to a lower limit value for the total damping of $\zeta = 0.00125$ for $Y_o \approx 5 \mu\text{m}$.

The analysis of the flux rate as a function of the coil tracks parameters reveals the possibility to obtain a further increase of the value of the magnetic flux rate by decreasing both the width and separation, and increasing the number of turns. With a value of $6 \mu\text{m}$ (minimum value compatible with high aspect ratio tracks, as

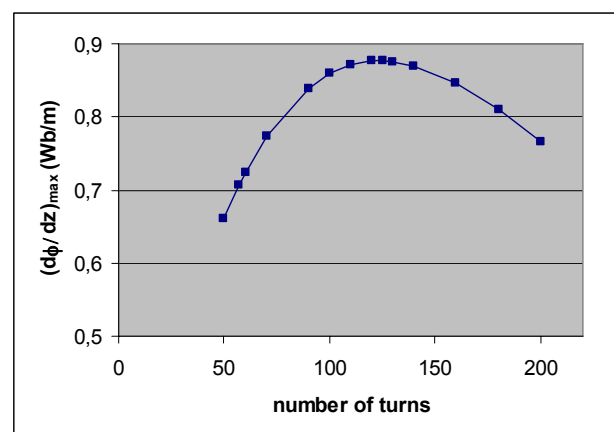


Figure 7. Maximum flux rate for coils with $6 \mu\text{m}$ metal track width and separation between metal tracks vs number of turns

explained later) for both width and separation of the tracks, a maximum flux rate is obtained for 120 turns (figure 7). However, this tends to increase the coil series resistance R_c , which can compromise the potential increase of the generated power related to the optimization of the flux rate.

Finally, as shown in equation (3), optimizing ζ_g requires reducing the value of R_c . This can be achieved by using a thicker metal for the coil tracks. For this, the selective growth of thick Cu tracks by electrochemical deposition [5] is proposed, in combination with a previous high aspect ratio lithography process. For 50 μm thick tracks, the series resistance of a device with the same design as our first prototype should drop down to a value of $R_c = 8.4 \Omega$. This would lead to an increase of two orders of magnitude in the generated power assuming the same conditions as in the previous case, obtaining a value of $P_L \geq 100 \mu\text{W}$.

According to these directives, figure 8 shows the simulation of an optimized device that includes a coil made of 50 μm thick, 6 μm pitch Cu tracks. For this design, the signal generated by the device has been calculated using the excitation conditions corresponding

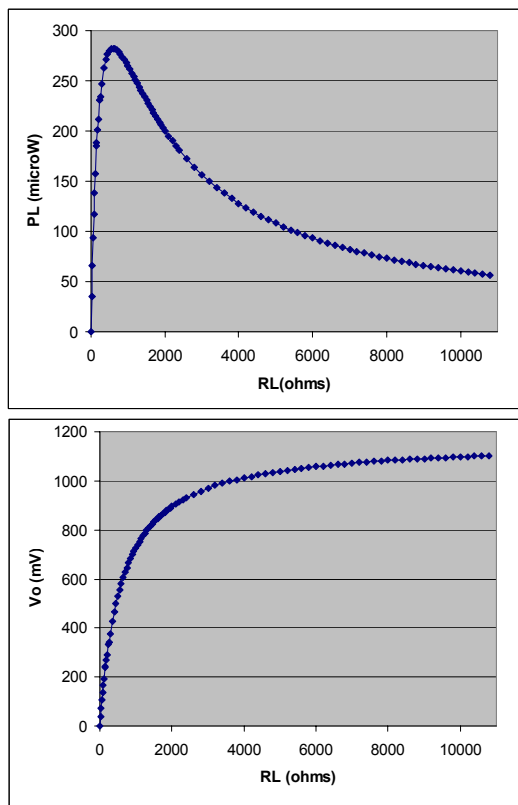


Figure 8. Generated P_L and V_o vs R_L calculated for the design with the highest flux rate ($n = 120$, $\zeta_p = 0.00125$, $f = 120 \text{ Hz}$, $Y_o = 4.4 \mu\text{m}$)

to the vibrations induced by a small microwave oven, $f = 120 \text{ Hz}$ and $Y_o = 4.4 \mu\text{m}$. As reported in [3], these are representative of the low level vibrations typically present in domestic and office environments, which have frequencies between 70 and 200 Hz and acceleration amplitudes between 1 and 10 m/s^2 . In this case, a maximum power of $P_{L,\text{opt}} = 282 \mu\text{W}$ is obtained with $R_L = R_{L,\text{opt}} = 600 \Omega$, with an amplitude of the output voltage of $V_o = 0.58 \text{ V}$. Increasing the load resistance up to $R_L = 1350 \Omega$ allows the generation of $P_L = 240 \mu\text{W}$ with a voltage amplitude $V_o = 0.8 \text{ V}$. It is interesting to remark that these voltage levels are compatible with the requirements related to the use of standard rectifying circuits for the generation of a DC signal suitable for power supply applications.

The comparison of these data with those reported in the literature for the same excitation conditions points out the possibility to generate similar power levels with the electromagnetic device proposed in this paper, obtaining higher values than with other approaches such as the electrostatic one. In this last case, Roundy et al [3] have reported a value of 43 μW from the simulation of an optimized design of electrostatic generator. These authors have also developed a prototype of piezoelectric generator, which gives a higher power of 70 μW . Simulations show that an optimized design would be capable of generating a power of 250 μW for the same vibration source, which is still slightly lower than the maximum value of $P_{L,\text{opt}} = 280 \mu\text{W}$ simulated for our optimized electromagnetic design. It is interesting to remark that the devices described in [3] correspond to designs with a total volume of 0.5 cm^3 , which is of the same order of magnitude as the volume that can be estimated for our device (in the range 0.6-0.7 cm^3).

5. CONCLUSIONS

In this work, we have presented the design and optimization of an electromagnetic inertial microgenerator for energy scavenging applications, compatible with Si technology.

The proposed design consists of a fixed micromachined coil and a movable magnet (inertial mass) mounted on a resonant structure (Kapton® membrane). The modeling of the device is based on a velocity damped resonator. The inclusion in the model of the losses related to the coil series resistance has allowed to analyze the design and loading conditions required to optimize both the generated power and output voltage, exploring the capabilities of this simple device structure for the development of devices suitable for practical applications.

According to this structure, a first prototype (not optimized) has been designed and fabricated. The

experimental mechanical and electrical characterization of this prototype has allowed the validation of the model developed for the inertial electromagnetic microgenerators, which is then used as a roadmap for a number of optimizations for the final device design.

These optimizations can be made in three main ways: decrease of the parasitic damping, geometric optimizations in order to maximize the magnetic flux rate $d\phi/dz$, and electric optimizations aiming at maximizing the electromagnetic coupling represented by the electromagnetic damping ζ_g . In relation to previous works proposing electromagnetic generators with a similar structure formed by a fixed coil and a movable magnet [3, 4], the simulation of the devices with the optimum design using the same excitation conditions as in these works reveals the possibility to obtain a significant increase of the flux rate (more than 2 orders of magnitude), thus allowing to generate much higher power levels.

For the optimum design, these results corroborate the ability of this devices to generate power up to hundreds of μW 's, with voltage levels compatible with the requirements related to the use of standard rectifying circuits for the generation of a DC signal suitable for power supply applications. This open interesting perspectives for the fabrication of power microgenerator suitable for their integration with advanced micro/nanosensors in microsystems for autonomous operation, wireless systems, or microsystem that must be completely embedded within the structure with no outside physical connections, allowing to overcome the limitations of conventional batteries in terms of miniaturization and devices lifetime.

ACKNOWLEDGEMENTS

The funding of this work by the IST program of the European Commission under the SENSATION project (ref. FP6-507231) is acknowledged by the authors from the University of Barcelona

REFERENCES

- [1] P.D. Mitcheson, T.C. Green, E.M. Yeatman, A.S. Holmes, "Architectures for vibration-driven micropower generators", *Journal of Microelectromechanical Systems* **13**, 429-440 (2004).
- [2] T. Sterken, K. Baert, C. Van Hoof, R. Puers, G. Borghs, P. Fiorini, "Comparative modeling for vibration scavengers", *Proceedings IEEE Sensors*, 2004.
- [3] S. Roundy, P.K. Wright, J. Rabaey, "A study of low level vibrations as a power source for wireless sensor nodes", *Computer Communications* **26**, 1131-1144 (2003).
- [4] C.B. Williams, C. Shearwood, M.A. Harradine, P.H. Mellor, T.S. Birch, R.B. Yates, "Development of an electromagnetic microgenerator", *IEE Proc. Circuits, Devices and Systems* **148**, 337-342 (2001).
- [5] S. Martínez, N. Yaakoubi, A. Pérez-Rodríguez, C. Serre, P. Gorostiza, J.R. Morante, J. Esteve, "Electrochemical deposition of metal layers and structures for Si-based microsystems", *Sensors and Actuators A* **99**, 41-44 (2002).
- [6] W.-S. Huang, K.-E. Tzeng, M.-C. Cheng, R.-S. Huang, "Design and fabrication of a vibrational micro-generator for wearable MEMS", *Proceedings of the 17th European Conference on Solid State Sensors Eurosensors XVII*, 695-697 (2003).